Characterization of mediastinal masses by MRI: Techniques and applications

Dania Daye, MD, PhD, and Jeanne B. Ackman, MD, FACR

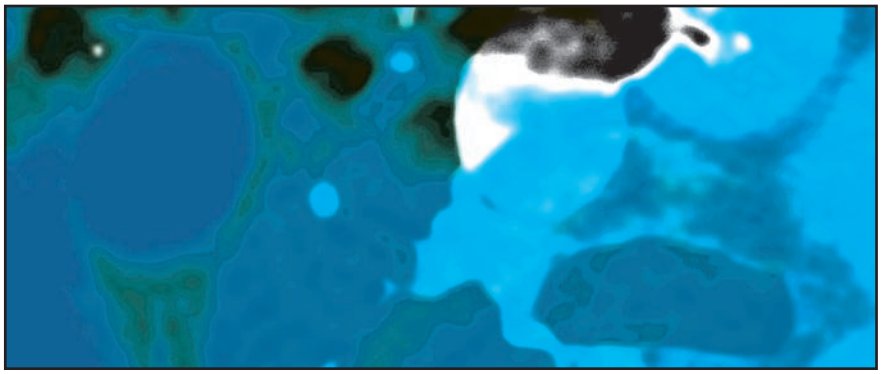

While chest computed tomography (CT) is the mainstay for initial evaluation of mediastinal masses detected incidentally by radiography or by clinical presentation, CT results are frequently indeterminate. Thoracic magnetic resonance imaging (MRI) offers a noninvasive way to further characterize mediastinal lesions, their site of origin, and their involvement of adjacent structures. Its higher soft-tissue contrast than CT yields superior tissue characterization and often provides more diagnostic specificity. Thoracic MRI has been shown to significantly alter clinical management, reduce the need for patient follow-up, and lower the surgical intervention rate.[1] Despite the advantages of thoracic MRI, however, the modality remains underutilized in the thorax[2] because of insufficient training, education, and awareness of its value.[3]

As is true elsewhere in the body, MRI allows improved differentiation of cystic from solid lesions and better distinction between simple and complex cystic lesions in the thorax. Chemical shift gradient echo MR imaging (in- and opposed-phase imaging) detects microscopic fat; fat-saturation techniques identify macroscopic fat. MRI can also identify the presence of blood products, smooth muscle, cartilage, and fibrous tissue within a lesion. Through the assessment of dynamic contrast enhancement (DCE) patterns and the extent of restricted diffusion, providing information about lesion vascularity, cellularity, and tissue architecture, MRI can further characterize various types of tissue. This article will discuss MR imaging technique and illustrate how the modality improves diagnostic specificity in mediastinal mass characterization by reviewing the features of selected mediastinal lesions and demonstrating how MR helps narrow the differential diagnosis, often to a single entity.

Dr. Daye is a radiology resident and Dr. Ackman is a radiologist at Massachusetts General Hospital, Boston, MA and an Assistant Professor at Harvard Medical School.

MRI Protocols

Basic lesion characterization with mediastinal MRI includes T1-weighted, T2-weighted, and pre-and post-dynamic contrast-enhanced (DCE) fat-saturated T1-weighted sequences. Ultrafast in- and opposed-phase chemical shift gradient echo (GRE) imaging is recommended for T1-weighted imaging because it provides a rapid means of T1-weighted imaging in a single breath-hold (~ 20 seconds) and provides additional information regarding the presence of microscopic or intravoxel fat. Breath-hold cardiac-gated double

Table 1. Mediastinal MRI Protocol

Pulse Sequence	GE	Siemens	Philips	Slice Thickness (mm)
Axial and Sagittal SSFP Balanced GRE	FIESTA	True FISP	BFFE	4-7
Coronal Ultrafast Spin Echo T2W	SSFSE	HASTE	UFSE	8
Sagittal Ultrafast Spin Echo Fat Sat T2W	SSFSE	HASTE	UFSE	7
Axial In- and Out-of-Phase Ultrafast GRE T1W	FSPGR	Turbo Flash	TFE	4
Axial Cardiac-Gated Double IR T2W (for T2-weighted imaging of a small area) OR	Double IR FSE T2	Double IR TSE T2	Double IR UFSE T2	4-7
Axial respiratory-Triggered, Radially Acquired T2W	PROPELLER	BLADE	MultiVane	4
Pre- and Post-3D Ultrafast GRE Fat Sat T1W with post-processed subtraction at 20 seconds (axial), 1 minute (axial), 3 minutes (sagittal), and 5 minutes (axial)	LAVA	VIBE	THRIVE	3-5
Optional Coronal and Sagittal STIR	FAST STIR	TURBO STIR	STIR TSE	7
Optional Diffusion-Weighted Imaging	eDWI	DWI	DWI	5-7
Optional Cardiac-Gated Double IR T1W	Double IR prep FSE T1	Double IR prep TSE T1	Double IR prep UFSE T1	4-7
Optional Cardiac-Gated Sagittal Double IR Fat Sat T2W	Double IR FSE T2 Fat Sat	Double IR TSE T2 Fat Sat	Double IR UFSE T2 Fat Sat	4-7

(GRE = gradient echo, IR = inversion recovery, STIR = short tau inversion recovery, Fat Sat = fat saturation, TR = repetition time, TE = echo time). TR, TE, Flip angles, etc. may vary by vendor/software package and should not be deemed sacrosanct. Slice thickness selection depends upon the size of the lesion and desired spatial resolution, allowing for trade-offs between signal and noise.)

Table 2. Noninvasive Thymic Lesion MRI Protocol

Non-Invasive Thymic Lesion MR Protocol
Axial Steady State Free Precession (SSFP)
Axial In- and Out-of-Phase Ultrafast Gradient Echo T1W
Axial Double IR T2W sequence (EKG-gated)
Optional: Pre- and Post-Gadolinium DCE 3D Ultrafast GRE Fat Sat T1W sequence at 20 seconds (axial), 1 minute (axial), 3 minutes (sagittal), and 5 minutes (axial)

T1W= T1-weighted, T2W=T2-weighted, IR: inversion recovery, DCE=dynamic contrast-enhanced, GRE=gradient echo

inversion recovery (IR) T2-weighted imaging provides high-signal, high-resolution images of the lesion of concern but should solely be used over a limited area, because it typically requires a ~20 second breath-hold *for each slice*, rather than for the whole pulse sequence, thereby taking minutes, rather than seconds to complete.

Repeated serial breath-holds can tire the patient, diminishing the patient's ability to cooperate for the remainder of the examination. When greater than ⅓ to ½ chest coverage is needed, it is usually better to perform respiratory-triggered, radially acquired (motion-corrected) T2-weighted images. These also take several minutes to acquire but enable the patient to rest and breathe quietly during image acquisition.

Supplemental EKG-gated double IR T2-weighted imaging can be performed afterwards over a prescribed, much more limited area, if needed to resolve any remaining question about, for example, lesion invasiveness. DCE imaging allows differentiation of lesions by

Table 3. Mediastinal Masses by Compartment (as classified by ITMIG)[4]

Prevascular Compartment (Anterior)	Visceral Compartment (Middle)	Paravertebral Compartment (Posterior)
Lymphadenopathy	Lymphadenopathy	Lymphadenopathy
Thyroid lesions	Thyroid lesions Aortic aneurysm Dilated pulmonary artery Aberrant subclavian arteries	Extramedullary hematopoiesis
Thymic lesions		
	Neurogenic tumors	Neurogenic tumors
		Lateral meningoceles
Germ cell tumors Pleuropericardial or mesothelial cysts	Mesothelial cysts Tracheal lesions Esophageal lesions	Mesothelial cysts
Morgagni hernia	Hiatal hernia Bronchogenic cysts Esophageal duplication cysts	Bochdalek hernia Neuroenteric cysts
Abscess	Abscess	Abscess
Hematoma	Hematoma	Hematoma
Fibrosing mediastinitis	Fibrosing mediastinitis	Fibrosing mediastinitis
Hemangioma	Hemangioma	Hemangioma
Lymphangioma	Lymphangioma	Lymphangioma
Sarcoma	Sarcoma	Sarcoma

Table 4. Computation of Chemical Shift Ratio and Signal Intensity Index

Chemical Shift Ratio (CSR)

$$CSR = \frac{OP\ SI\ THYMUS\ /\ OP\ SI\ PARASPINAL\ MUSCLE}{IP\ SI\ THYMUS\ /\ IP\ SI\ PARASPINAL\ MUSCLE}$$

- CSR ≤ 0.7 corresponds to normal or hyperplastic thymus, rather than tumor
- CSR of ≥ 1.0 corresponds to tumor, in most but not all cases
- CSRs of 0.8 and 0.9 are indeterminate

Signal Intensity Index (SII)

$$SII = \frac{(IP\ SI\ THYMUS - OP\ SI\ THYMUS) \times 100}{IP\ SI\ THYMUS}$$

- SII > 9% corresponds to normal thymus or thymic hyperplasia, rather than tumor

(IP = in-phase, OP = opposed-phase, SI = signal intensity as measured by ROI)

their enhancement pattern and enables post-processed subtraction, the latter of which is a very useful tool in cases of subtle lesion enhancement, especially when the lesion is T1-hyperintense on pre-contrast images.

Supplemental pulse sequences can be performed when necessary for a particular case. These include fat-saturated T2-weighted imaging, diffusion-weighted imaging (DWI) to assess the presence and degree of restricted diffusion, and short *tau* inversion recovery (STIR) imaging, the latter being the most sensitive pulse sequence for bone marrow edema. When prescribing an MRI protocol, one should always strive to limit the patient's time spent in the magnet to that solely required for diagnosis, in order to optimize the patient experience and keep the MR schedule running on time.

Breath-hold imaging is superior to respiratory gating for elimination of

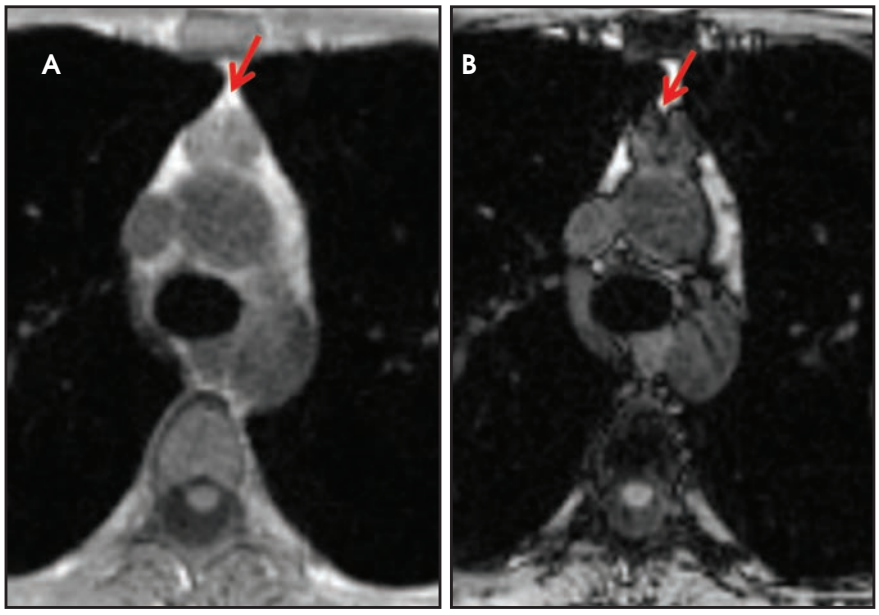

FIGURE 1. *Differentiating thymic hyperplasia from thymoma in a 38-year-old asymptomatic woman. There is bipyramidal, intermediate T1 signal tissue in the thymic bed on the in-phase T1-weighted (T1W) image (A) with significant suppression on the opposed-phase image (B). These MR signal characteristics and morphology are compatible with mild thymic hyperplasia for age, rather than a thymic tumor, such as a thymoma.*

respiratory motion artifact. Technologist proficiency with breath-hold technique and a breath-hold rehearsal with the patient prior to scanning are critical to success of this approach. We have found adults of all ages up through their early '90s capable of serial breath-holds for up to 20 seconds. Longer breath-holds can be challenging and affect image quality because poor breath-holds yield respiratory motion artifact. Therefore, breath-hold MR pulse sequences should be tailored to take 20 seconds or less, adjusting slice thickness, number of excitations, and/or other parameters as needed. For pre-contrast imaging, we employ slice thicknesses ≥ 4 mm because thinner slices generally have an unacceptable signal-to-noise ratio (SNR). For pre- and post-contrast 3D-ultrafast gradient echo fat-saturated imaging, slice thicknesses as thin as 3 mm can generally be used with success.

If difficulty is anticipated, two liters of nasal cannula oxygen (or more if the patient is on oxygen at baseline) can enhance breath-holding capability.[4] When cardiac gating is required due to lesion location, we employ electrocardiogram (EKG) gating, rather than peripheral cardiac gating to more reliably eliminate pulsatility artifact. See two sample MR imaging protocols in Tables 1 and 2. Table 1 (Mediastinal MRI Protocol) can used to evaluate all mediastinal masses, while Table 2 (Non-invasive Thymic Lesion MRI Protocol) is a more curtailed and efficient protocol that can be used to evaluate noninvasive-appearing thymic and other suitable lesions.

Mediastinal masses by compartment

Mediastinal masses are stratified by mediastinal compartment, as recently re-defined by the International Thymic Malignancy Interest Group (ITMIG) on the basis of CT, rather than chest radiography (CXR).[5] The prevascular (anterior) mediastinal compartment includes structures anterior to the pericardium and ascending aorta. The visceral (middle) mediastinal compartment includes all mediastinal structures extending from the anterior pericardium to a vertical line drawn 1 cm posterior to the anterior margin of the spine, including the trachea, esophagus, heart, and thoracic aorta. The paravertebral (posterior) mediastinal compartment includes all mediastinal structures posterior to this vertical line, with the lateral extent along the lateral margin of the transverse processes of the thoracic spine. A list of the mediastinal masses that typically arise within each compartment is provided in Table 3.

Prevascular (anterior) mediastinal compartment

The anterior mediastinum includes the following structures: thymus, lymphatic tissue, left innominate vein, and fat. Various prevascular mediastinal masses arise from these structures and are listed in Table 3. The discussion that follows will cover ways to distinguish these lesions from one another and how MR contributes to diagnostic specificity.

Differentiating thymic lesions

Once a thymic lesion is detected, a key task for the radiologist is to distinguish thymic lesions that do not require surgical intervention (thymic hyperplasia, thymic cysts, and lymphoma) from those necessitating resection (non-lymphomatous thymic tumors). The differentiating CT imaging features of each of these entities have been previously discussed.[6] We will review some of them here.

The normal adult thymus is usually triangular/bipyramidal/arrowheaded, or quadrilateral in shape. While a maximal thymic lobar thickness of 1.3 cm was reported in patients older than 20 years of age in the 1980s,[7] this maximal thymic lobar thickness measurement has been more recently adjusted upward in the 20-30-year age group and is often greater in young women than in young men. Thymic attenuation also tends to be greater in young women than young men. The maximal thymic lobar thickness for triangular thymuses in adults aged 20-30 years is 1.6 cm and for quadrilateral thymuses is 2.2 cm.[8] Awareness of variation in thymic size and attenuation based on sex and age is important to avoid misinterpretation of normal thymus as thymic hyperplasia or, even more critically, as thymic neoplasm. On CT, thymic

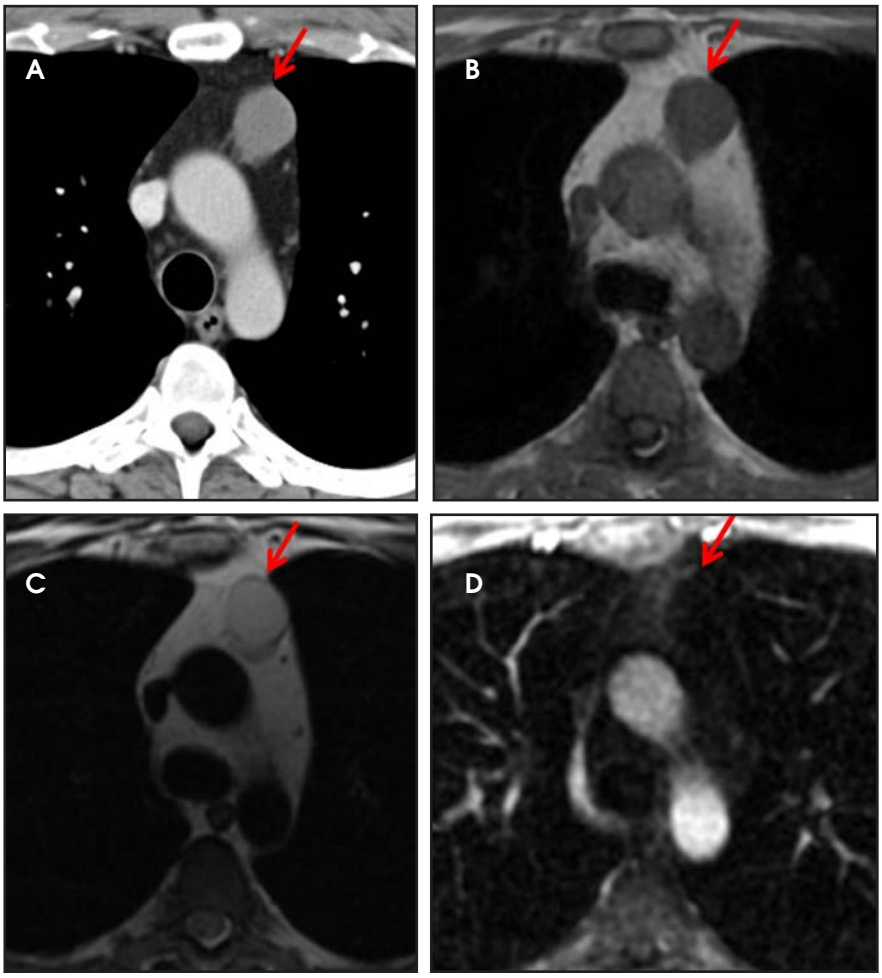

FIGURE 2. *Differentiating a hyperattenuating thymic cyst from thymic neoplasm in a 41-year-old man with an incidentally found, indeterminate, hyperattenuating thymic lesion on chest CT. (A). MRI reveals a homogeneously T1-isointense (B), T2-hyperintense (C), well-circumscribed, ovoid mass in the thymic bed at the level of the aortic arch. The lesion demonstrates no internal enhancement and thin, smooth wall enhancement on the post-contrast image (D). These MRI findings are consistent with a thymic cyst.*

hyperplasia can sometimes be difficult to differentiate from thymic neoplasm. Because the normal thymus involutes and becomes fattier with age, chemical shift MRI can be used to determine if *microscopic* fat is present throughout the tissue. Qualitative evaluation of suppression on out-of-phase images is not as sensitive as quantitative assessment. If the thymic tissue suppresses on out-of-phase images, with a chemical shift ratio (CSR) of ≤ 0.7 or a signal intensity index (SII) ≥ 9%, the thymic tissue is either normal or hyperplastic, depending upon the age of the patient and the expected thymic thickness for age (Figure 1 and Table 4).[9,10] Please note: cases of non-suppressing normal thymus and thymic hyperplasia have been reported.[10,11]

Therefore, while the finding of suppression on opposed-phase images generally confirms the presence of normal or hyperplastic thymus, the absence of suppression does not absolutely rule out thymic hyperplasia. If the remaining features of the thymic tissue (morphology and signal—intermediate T1 signal, mildly T2-hyperintensity to muscle) still raise the possibility of thymic hyperplasia, rather than tumor, consider performing a follow-up MRI in 3-6 months to confirm stability, regression, and/or increasing suppression of the tissue over time, with the aim to spare the patient unnecessary thymectomy.

MRI is superior to CT in reliably distinguishing cystic from solid lesions. The differential diagnosis for a hyperattenuating (up to 100 Hounsfield units), well-circumscribed, round, ovoid, or saccular homogeneous attenuation, prevascular lesion on CT includes a benign hemorrhagic or proteinaceous thymic cyst and a solid thymic lesion. These lesions are often misinterpreted as thymomas and lymph nodes on CT because of their apparent solid nature, often resulting in unnecessary thymectomy.[12] On MRI, a thymic cyst exhibits homogeneous but variable T1 signal depending on its serous, proteinaceous, or hemorrhagic nature, homogeneous and usually, marked T2-hyperintensity (isointense to cerebrospinal fluid), with no internal enhancement. It may be unilocular or multilocular. Thin, smooth wall enhancement may be present (Figure 2). Thymic MRI can detect complex cysts by identifying enhancing mural nodularity, wall thickening, and septations that may be undetectable by CT secondary to CT's lower soft tissue contrast.[13,14] We perform serial follow-up MR of thymic cysts, initially at 6 months, and then annually for 5 years to ensure continued benign features. To date, we have observed no malignant transformation of these lesions. Complex cysts (with abnormal, irregular, and/or nodular wall thickening and septations), can be followed or resected, depending upon the level of radiologic and clinical concern—their differential diagnosis includes benign inflammatory lesions and cystic thymic neoplasms. Solid thymic lesions are readily identified and characterized on MRI using T1-weighted, T2-weighted, DCE, and occasionally DWI sequences.[15] Solid lesions are almost always resected, unless lymphoma is suspected.

Differentiating lymphoma from thymoma

On CT and MRI, mediastinal lymphoma tends to exhibit lobulated and multinodular morphology secondary to coalescence of multiple lymph nodes. Lymphoma also more commonly

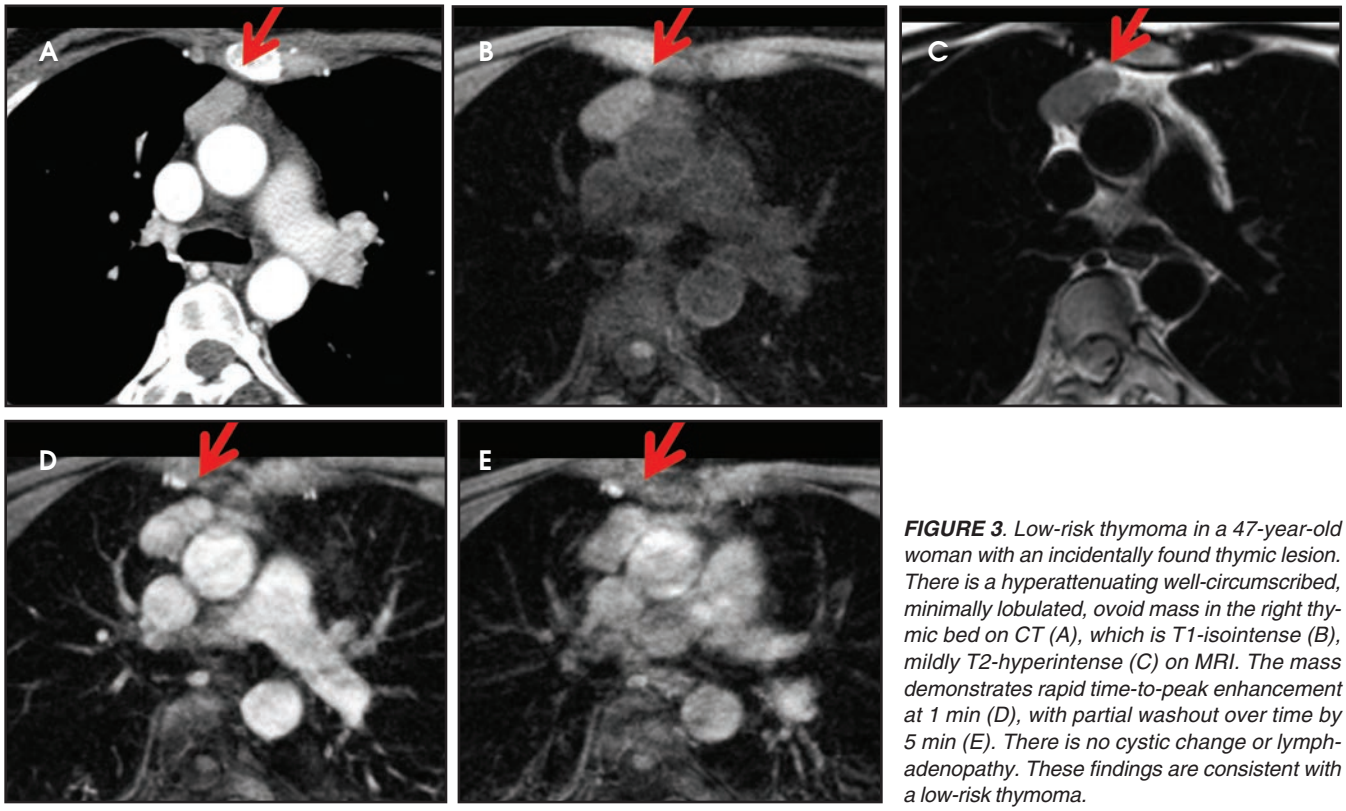

***FIGURE 3**. Low-risk thymoma in a 47-year-old woman with an incidentally found thymic lesion. There is a hyperattenuating well-circumscribed, minimally lobulated, ovoid mass in the right thymic bed on CT (A), which is T1-isointense (B), mildly T2-hyperintense (C) on MRI. The mass demonstrates rapid time-to-peak enhancement at 1 min (D), with partial washout over time by 5 min (E). There is no cystic change or lymphadenopathy. These findings are consistent with a low-risk thymoma.*

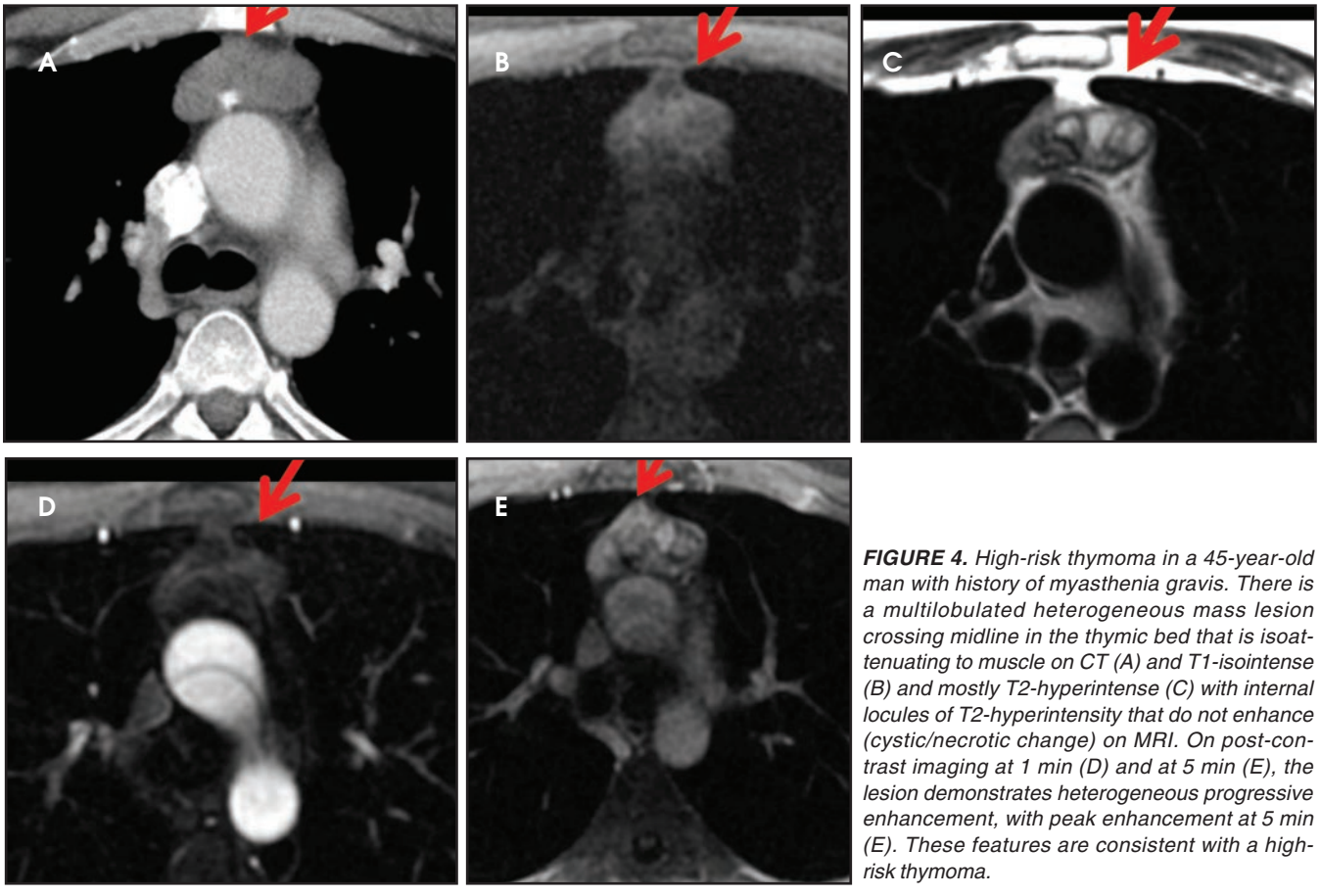

***FIGURE 4.** High-risk thymoma in a 45-year-old man with history of myasthenia gravis. There is a multilobulated heterogeneous mass lesion crossing midline in the thymic bed that is isoattenuating to muscle on CT (A) and T1-isointense (B) and mostly T2-hyperintense (C) with internal locules of T2-hyperintensity that do not enhance (cystic/necrotic change) on MRI. On post-contrast imaging at 1 min (D) and at 5 min (E), the lesion demonstrates heterogeneous progressive enhancement, with peak enhancement at 5 min (E). These features are consistent with a high-risk thymoma.*

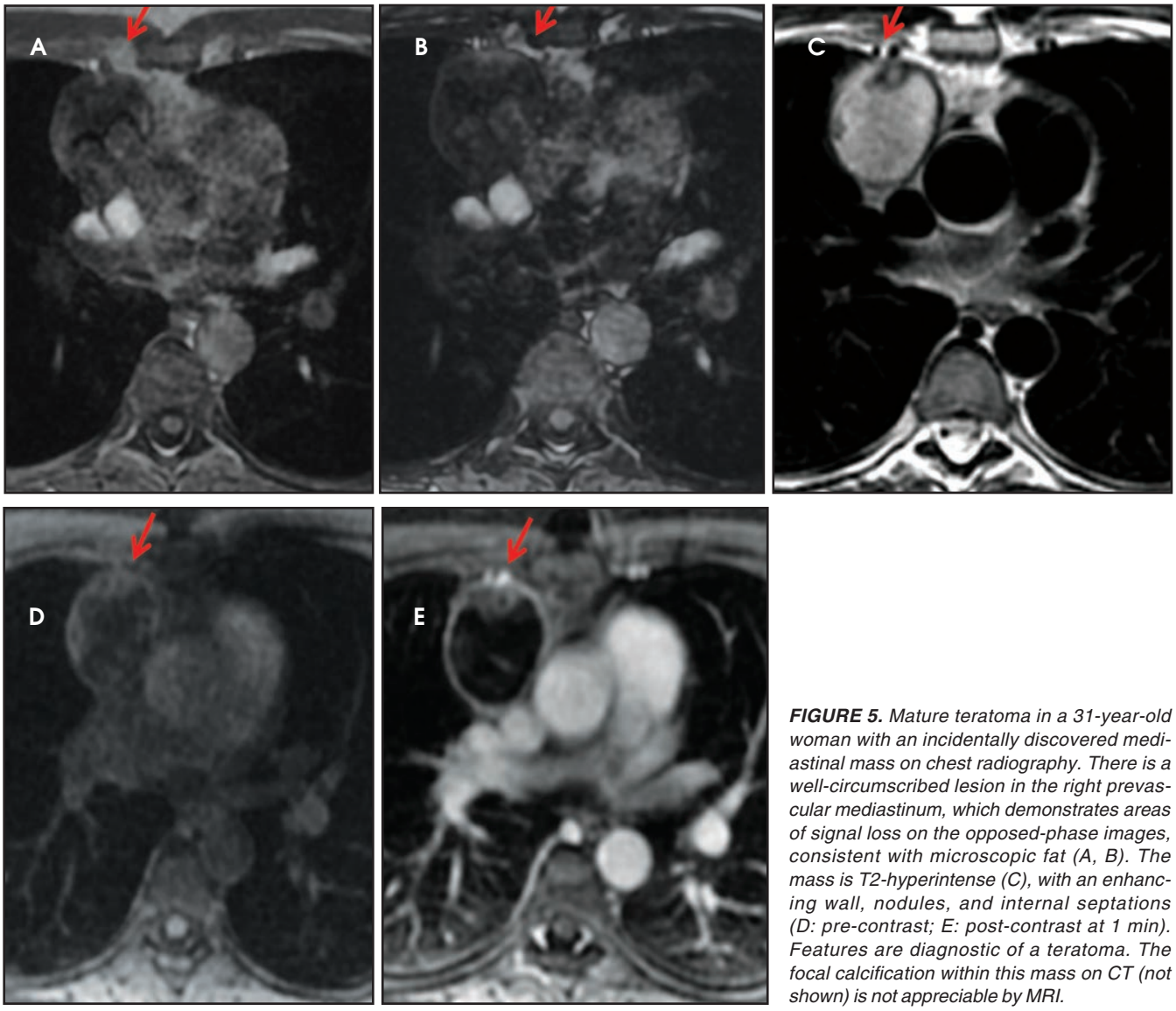

FIGURE 5. *Mature teratoma in a 31-year-old woman with an incidentally discovered mediastinal mass on chest radiography. There is a well-circumscribed lesion in the right prevascular mediastinum, which demonstrates areas of signal loss on the opposed-phase images, consistent with microscopic fat (A, B). The mass is T2-hyperintense (C), with an enhancing wall, nodules, and internal septations (D: pre-contrast; E: post-contrast at 1 min). Features are diagnostic of a teratoma. The focal calcification within this mass on CT (not shown) is not appreciable by MRI.*

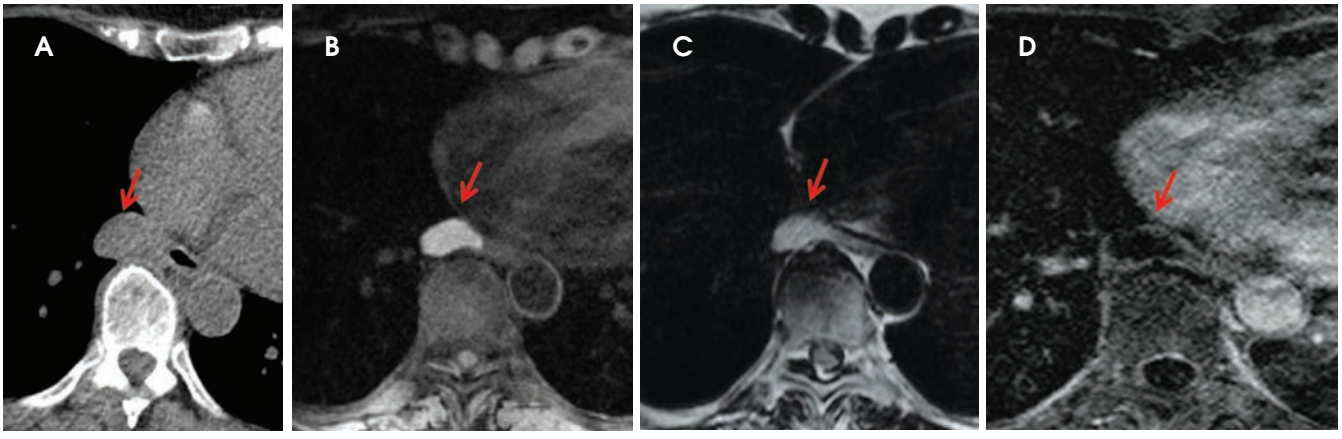

FIGURE 6. *Foregut duplication cyst in a 77-year-old woman with history of neurofibromatosis type 1 and an incidentally discovered mediastinal mass. There is a well-circumscribed right paraesophageal lesion on CT (A). On MRI, the lesion is T1-hyperintense (B), T2-hyperintense (C), with thin smooth-wall enhancement and no internal enhancement on the post-contrast subtraction image (D). These findings are consistent with a foregut duplication cyst.*

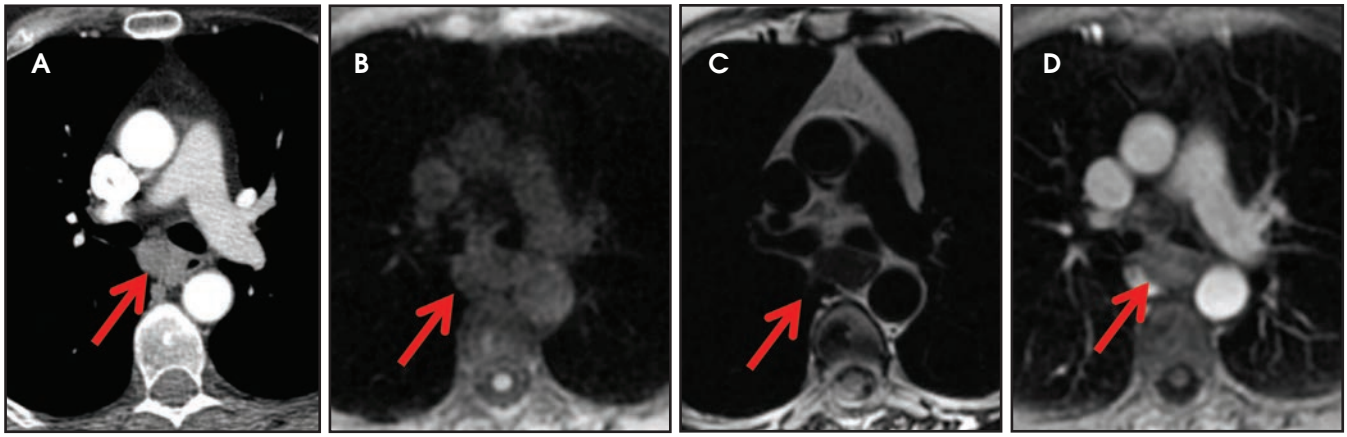

FIGURE 7. *Esophageal leiomyoma in a 66-year-old woman with an incidentally discovered mediastinal mass. There is a well-circumscribed, homogeneous attenuation, ovoid mass within the posterior mediastinum on CT (A). The mass compresses the mid-esophagus, with no fat plane between the mass and the esophagus. On MRI, the mass is of intermediate T1 signal (B), of relatively low T2 signal (C) compared to typical lymph nodes and malignant neoplasms, and mildly enhances (D). These features, and, in particular, the low T2 signal, favor an esophageal leiomyoma over lymphadenopathy and esophageal cancer.*

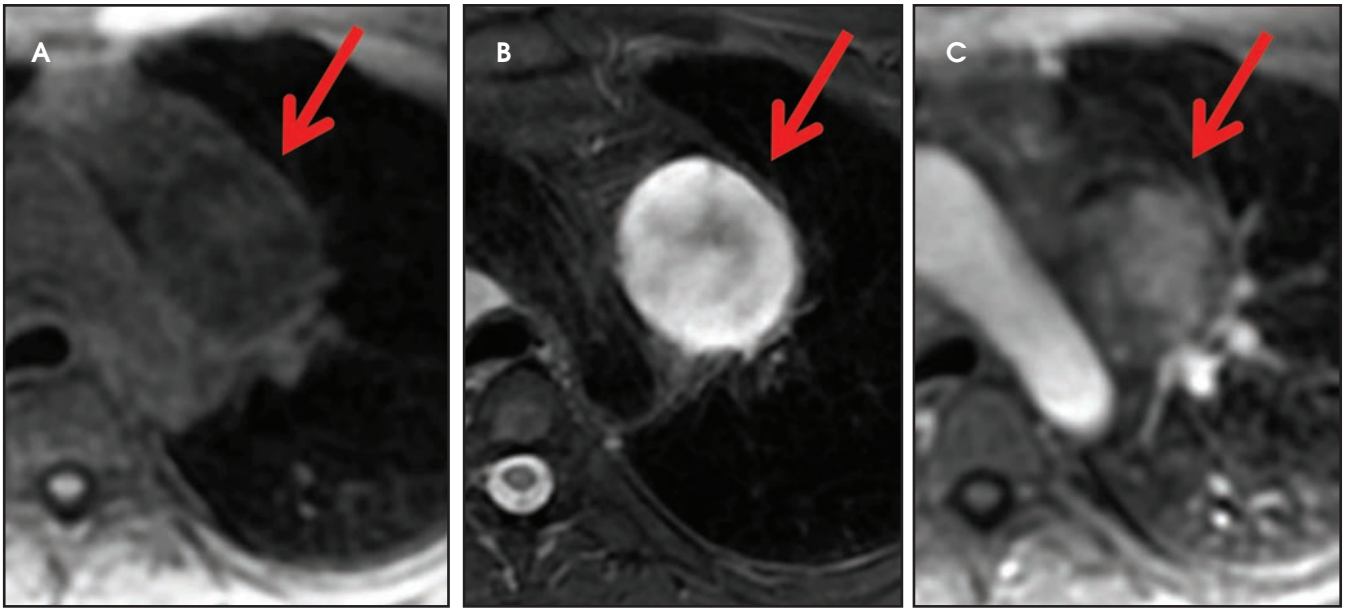

FIGURE 8. *Neurofibroma in a 39-year-old man with history of neurofibromatosis type 1. There is a T1-hypointense (A) lesion in the left visceral mediastinum in the expected location of the either the vagus, recurrent laryngeal, or phrenic nerve. The lesion exhibits peripheral T2-hyperintensity and central T2-hypointensity (B) and demonstrates mild enhancement, without evidence of cystic change or hemorrhage (C). These features are consistent with a neurofibroma, rather than schwannoma. Paragangliomas, thymomas, and lymphoma have not been reported to exhibit this target sign and enhance far more, with paraganglioma the most vigorously enhancing of these lesions.*

exerts mass effect on adjacent mediastinal structures and involves pericardium more often than thymoma.[16] Thymoma more typically presents as a rounded, off-midline thymic mass. When advanced, thymoma becomes more lobulated and may cross midline, as is often the case with lymphoma. When thymoma and lymphoma are considerations in the differential diagnosis of an anterior mediastinal lesion, mediastinal MRI can help differentiate the two entities and can better assess pericardial involvement—the latter is important for staging and surgical planning. Thymomas may exhibit characteristic DCE patterns on MRI (Figure 3), although there are apt to be exceptions.[17] Specifically, low-risk thymomas typically exhibit more rapid mean time-to-peak enhancement (1.3 minutes) when compared to high-risk thymomas (2.5 minutes) (Figure 4) and non-thymomas (3.2 minutes) including thymic carcinoma, lymphoma, germ cell tumors, and neuroendocrine tumors.[18] An attempt at distinction between low-risk and high risk thymomas and thymic carcinoma can also be made with DWI and apparent diffusion coefficient (ADC) mapping. High-risk thymomas generally exhibit lower ADC values than low-risk thymomas, with a proposed ADC cutoff value

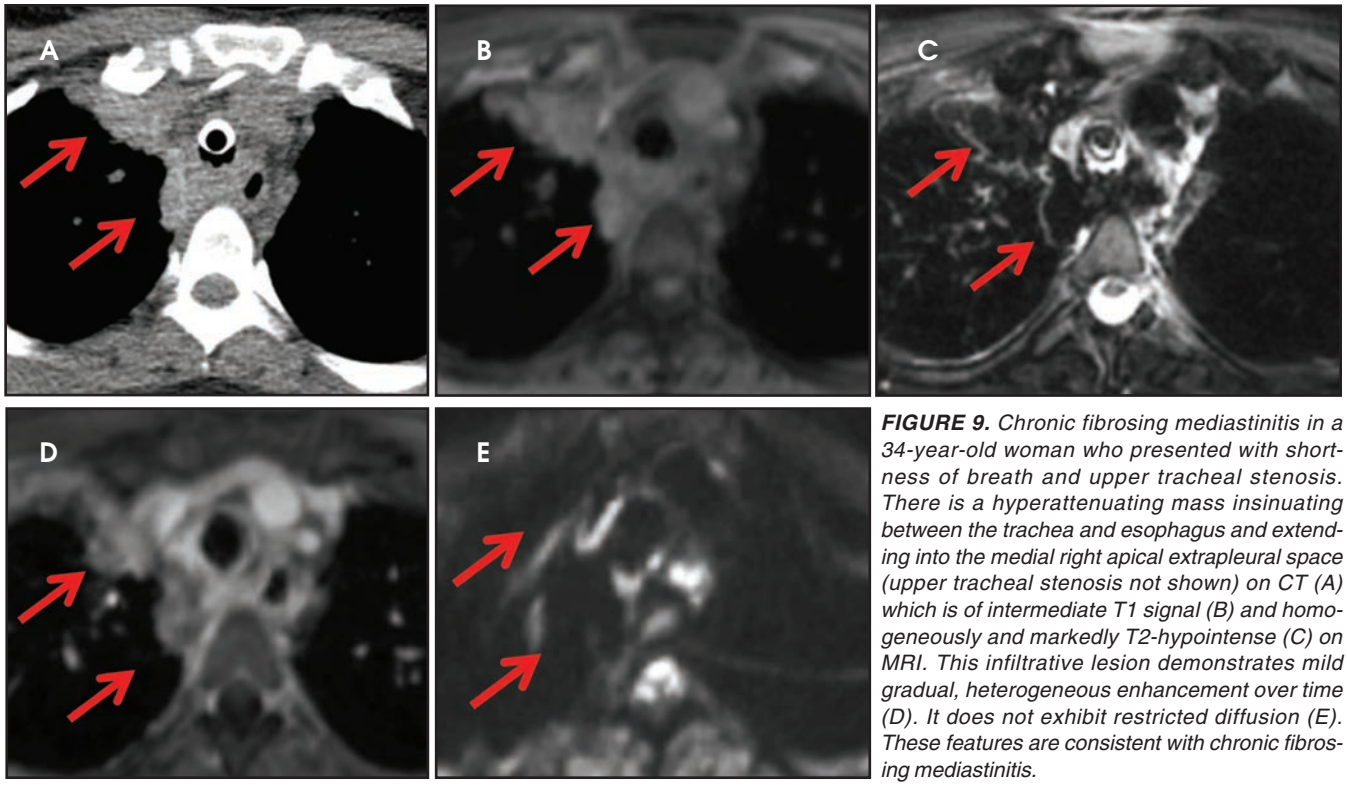

FIGURE 9. *Chronic fibrosing mediastinitis in a 34-year-old woman who presented with shortness of breath and upper tracheal stenosis. There is a hyperattenuating mass insinuating between the trachea and esophagus and extending into the medial right apical extrapleural space (upper tracheal stenosis not shown) on CT (A) which is of intermediate T1 signal (B) and homogeneously and markedly T2-hypointense (C) on MRI. This infiltrative lesion demonstrates mild gradual, heterogeneous enhancement over time (D). It does not exhibit restricted diffusion (E). These features are consistent with chronic fibrosing mediastinitis.*

of 1.56 x 10^{-3} mm^2/second.[19] This cut-off value should only be used as a rough guide, as it can vary by MR vendor, MR software, and other factors.

Differentiating fat-containing anterior mediastinal masses

Thymolipomas, liposarcomas, and mature teratomas are anterior mediastinal masses that usually contain macroscopic or gross fat. Macroscopic fat is readily appreciable on both CT and MRI. On MRI, the combination of T1/T2-hyperintensity and saturation on fat-saturated MRI pulse sequences proves the presence of macroscopic or gross fat. Mature teratomas or dermoid cysts are the most common germ cell tumor of the mediastinum and may contain macroscopic and/or microscopic fat. A fat-fluid level within an anterior mediastinal mass is virtually diagnostic of a teratoma, indicating the presence of sebum (Figure 5).[20,21] Both thymolipomas and liposarcomas are quite rare. Thymolipomas arise from thymic tissue, contain both macroscopic fat and strands of thymic tissue, typically conform to adjacent anatomic structures, and are noninvasive.[22] In contrast, liposarcomas tend to insinuate between and splay mediastinal structures, with greater amounts of non-fatty soft tissue content usually indicative of higher tumor grade.[23,24]

Visceral (middle) mediastinal compartment

The visceral mediastinal compartment contains the following structures: central airways, esophagus, lymph nodes, lymphatics, heart, great vessels, and nerves, with associated paraganglia. Various mediastinal masses arise from these structures and are listed in Table 3. The discussion that follows covers ways in which these lesions can be distinguished from one another and how MRI contributes to diagnostic specificity.

Foregut duplication cysts

Foregut duplication cysts and more specifically, bronchogenic and esophageal duplication cysts are among the most common visceral mediastinal lesions besides lymphadenopathy. While CT can be fairly diagnostic when they are of water attenuation, CT is indeterminate when they are of higher attenuation and mimic solid lesions. Bronchogenic cysts have been shown to have attenuation values of up to 100 HU on account of proteinaceous, hemorrhagic, and/or calcium oxalate content (Figure 6). MRI reliably distinguishes between cystic and solid lesions. Foregut duplication cysts are typically well-circumscribed, round (bronchogenic cysts), or tubular (esophageal duplication cysts), homogeneous in CT attenuation and MRI signal, and in close proximity to the central airways or esophagus.[25] On MRI, foregut duplication cysts exhibit variable, but homogeneous T1 signal, depending upon the nature of the fluid, marked T2-hyperintensity, and either no enhancement or thin, smooth wall enhancement.[26] The differential diagnosis for foregut duplication cysts includes lymphangiomas and mesothelial (pleuropericardial) cysts.[27]

Esophageal neoplasms

Chest CT is currently the initial cross-sectional imaging modality of choice for the evaluation of esophageal neoplasms.[28,29] Upper endoscopy remains the standard means of esophageal

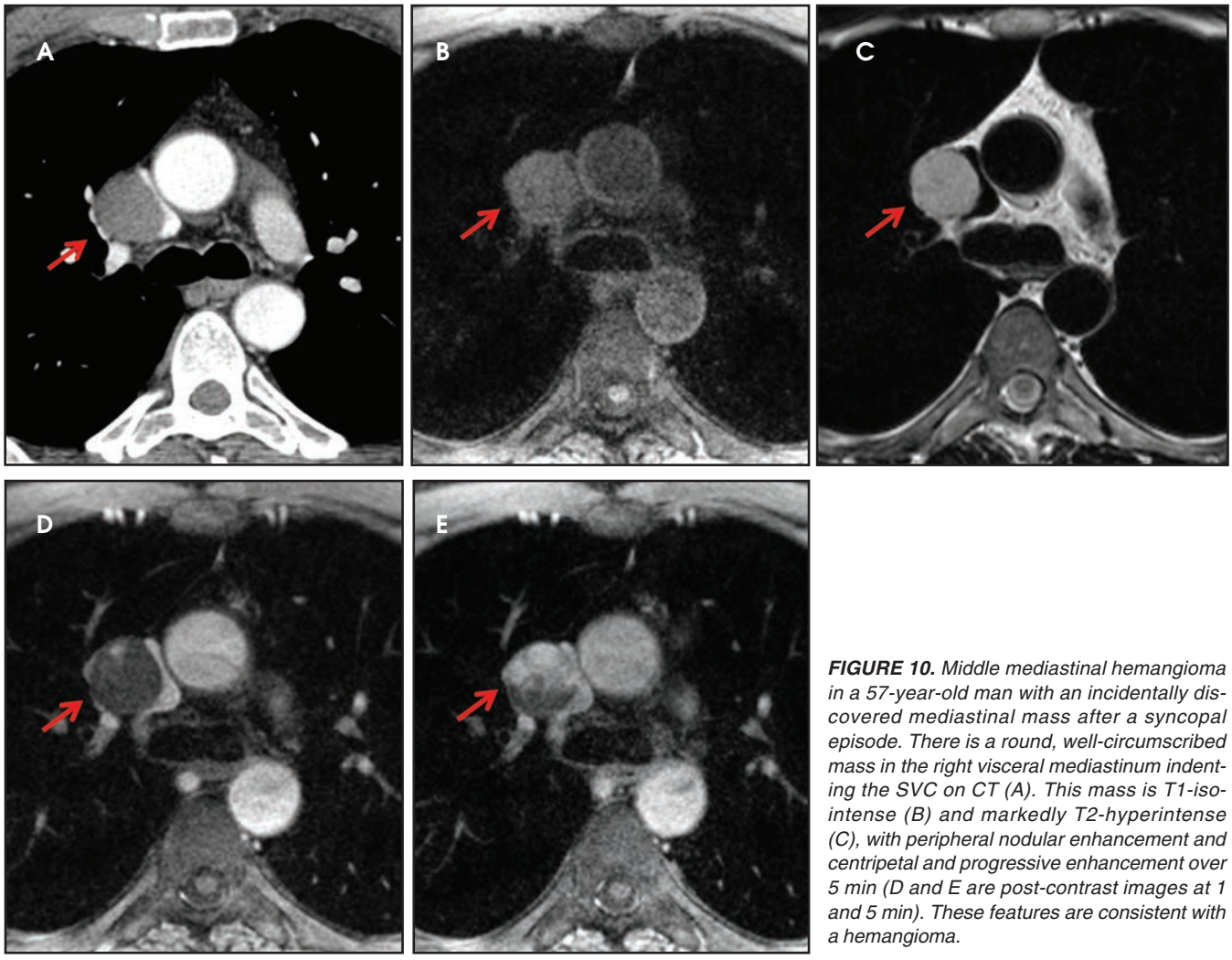

FIGURE 10. *Middle mediastinal hemangioma in a 57-year-old man with an incidentally discovered mediastinal mass after a syncopal episode. There is a round, well-circumscribed mass in the right visceral mediastinum indenting the SVC on CT (A). This mass is T1-isointense (B) and markedly T2-hyperintense (C), with peripheral nodular enhancement and centripetal and progressive enhancement over 5 min (D and E are post-contrast images at 1 and 5 min). These features are consistent with a hemangioma.*

lesion sampling and diagnosis. Mediastinal MRI can be used when lesion characterization by CT is indeterminate. Specifically, MRI can better delineate the composition of a lesion, its location, its relationship to adjacent structures, and whether or not it invades other mediastinal compartments. This additional information may be critical for patient management. Esophageal tumors include esophageal carcinoma, esophageal metastases, and less commonly esophageal leiomyoma. Typically, primary esophageal carcinomas and metastatic lesions present as an asymmetric thickening of the esophageal wall. MR findings of esophageal leiomyoma are virtually diagnostic when a round, well-circumscribed, exophytic, homogeneously low-to-intermediate T1/T2 signal mass with gradual enhancement on dynamic contrast-enhanced images is seen (Figure 7). Involvement of the various layers of the esophageal wall by malignant primary or metastatic tumors is best detected on high-resolution T2-weighted images with a small field-of-view (FOV), using a spinal coil,[30] or with a larger FOV, using a spinal coil and torso coil combination.

Paragangliomas and nerve sheath tumors

Paragangliomas or extra-adrenal pheochromocytomas, while rare, most commonly arise in the middle mediastinum from the aortopulmonary paraganglia.[31] MRI can aid in the differentiation of these tumors from lymph nodes and other mediastinal masses; they are typically indeterminate on CT. On MRI, paragangliomas are usually markedly T2-hyperintense and demonstrate vivid enhancement.[32,33] Larger paragangliomas may exhibit a "salt and pepper" appearance on T2-weighted images due to vascular flow voids in these hypervascular tumors.[32] Nerve sheath tumors in the visceral mediastinum can arise from the phrenic, vagus, or recurrent laryngeal nerves which pass through this mediastinal compartment (Figure 8). Additional discussion of the MRI appearance of nerve sheath tumors is included in the posterior mediastinal section below.

Fibrosing mediastinitis

Fibrosing mediastinitis may be focal or infiltrative and can mimic neoplasm. When infiltrative, it may encase and narrow adjacent mediastinal structures.[34] When acute, mediastinitis demonstrates T2-hyperintensity. When

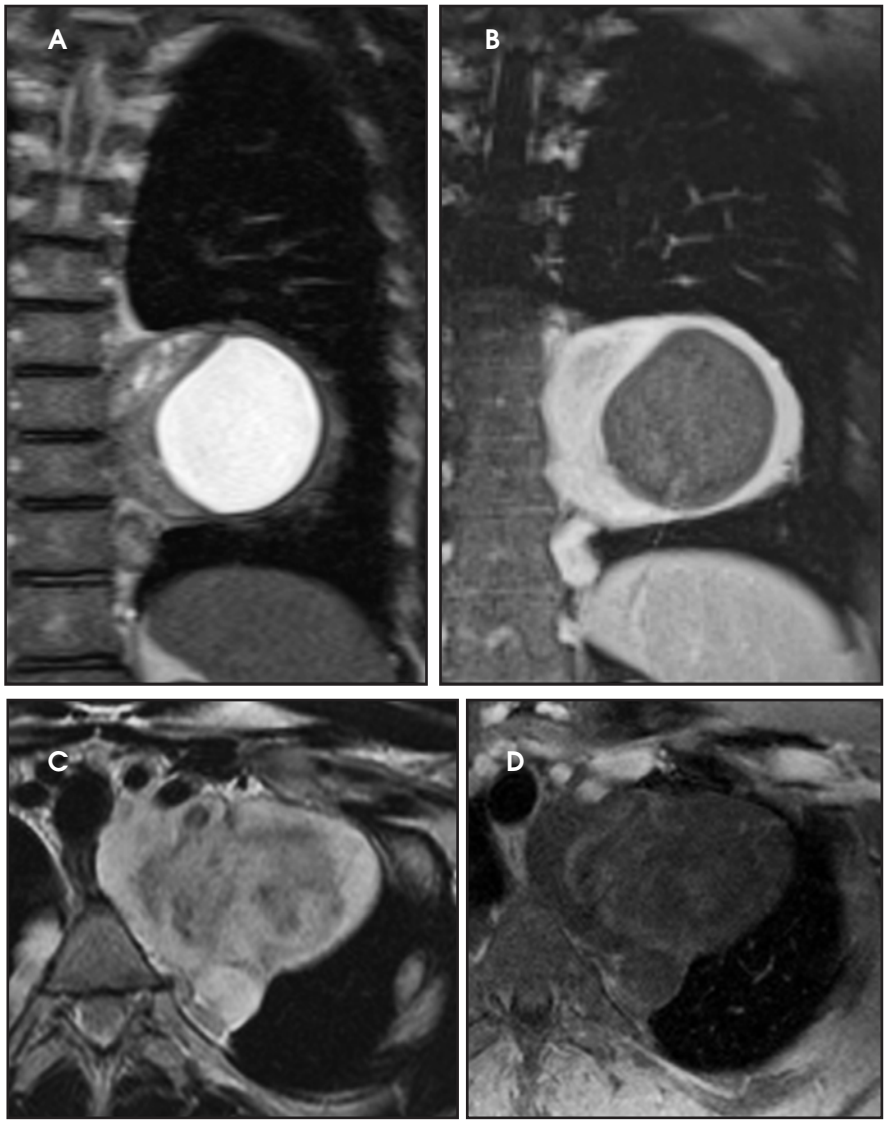

FIGURE 11. *Differentiating mediastinal nerve sheath tumors by MRI. These tandem left paravertebral schwannomas (A, B) on coronal T2-weighted MRI are round, well-circumscribed, and centrally T2-hyperintense, with relative peripheral T2-hypointensity, whether partially cystic (upper lesion) or solid (lower lesion) (A). There is substantial enhancement of their solid component (B). In contrast, this left paravertebral neurofibroma (C, D), while also well-circumscribed, exhibits a "target sign" on T2-weighted images, with central T2-hypointensity and peripheral T2-hyperintensity (C), and very mild enhancement (D).*

chronic, the collagenous or fibrous material in this lesion yields T2-hypointensity, whether or not there is concurrent calcification, distinguishing it from most neoplasms, which are typically T2-hyperintense to muscle (Figure 9).

Mediastinal lymphangiomas and hemangiomas

Lymphangiomas often present as unilocular or multilocular cysts, however they may contain enhancing, solid components.[35] CT typically demonstrates a multilocular cystic mass in the mediastinum, which can be of water attenuation or higher attenuation, mimicking a solid lesion and often requiring further characterization. Hemangiomas can be difficult to definitively diagnose on CT imaging, as most chest CT studies are performed without dynamic contrast-enhanced imaging, on account of the excessive ionizing radiation exposure it would impose. Dynamic contrast-enhanced MRI can help diagnose this entity without ionizing radiation. Mediastinal hemangiomas can demonstrate peripheral nodular enhancement and fill-in or partial fill-on over time, similar to liver hemangiomas (Figure 10), but not always. It is possible that this enhancement pattern is more reliably found in lesions larger than 1.5 centimeters, as is true in the liver.[36-40]

Paravertebral (posterior) mediastinal compartment

The paravertebral compartment includes lymph nodes, lymphatics, nerve tissue, and the thoracic duct. Various mediastinal masses arise from these structures and are listed in Table 1. Other than lymphadenopathy, neurogenic tumors are among the most common lesions in this compartment and are discussed below.

Differentiating neurofibromas from schwannomas

Nerve sheath tumors arising in the paravertebral mediastinum include neurofibromas and schwannomas, which have a similar appearance on CT. MRI allows better differentiation of these lesions. Specifically, neurofibromas are typically T2-hypointense centrally with peripheral T2-hyperintensity, yielding a characteristic "target appearance" (Figure 8).[32] Neurofibromas are nonencapsulated, usually exhibit limited enhancement, and rarely contain cystic components. Cystic change and more rapid or vivid enhancement in a neurofibroma on CT or MR should increase concern for malignant transformation—MR may better highlight these features that raise the likelihood of malignancy because of its higher soft tissue contrast. Schwannomas, on the other hand, are encapsulated, are typically T2-hyperintense centrally, whether or not they are partially cystic, and their solid components moderately enhance (Figure 11).[41]

Other neurogenic tumors

Other neurogenic tumors in the posterior mediastinum include paragangliomas along paravertebral sympathetic

ganglia (MRI appearance discussed above in Visceral Mediastinum section), ganglioneuromas, ganglioneuroblastomas, and neuroblastomas, with the latter two entities more commonly presenting in the pediatric population. On MRI, ganglioneuromas exhibit T1-isointensity or -hypointensity to muscle, heterogeneous T2 signal , and occasionally a "whorled appearance" on account of its distinctive tumor architecture.[41] Neuroblastomas and ganglioneuroblastomas are more aggressive tumors with a variable appearance on MRI, may contain hemorrhagic foci, and can metastasize.[32]

Conclusion

While CT imaging remains the modality of choice for initial cross-sectional imaging evaluation of mediastinal lesions, thoracic MRI provides more thorough and often definitive evaluation of mediastinal masses because of its superior tissue characterization and its better delineation of the relationship of a mass to adjacent anatomic structures.[1] The use of thoracic MRI in the appropriate clinical setting has the potential to improve clinical diagnosis and patient management and reduce overall health care costs, by eliminating unnecessary intervention and follow-up.

References

1. Ackman JB, Gaissert HA, Lanuti M, et al. Impact of Nonvascular Thoracic MR Imaging on the Clinical Decision Making of Thoracic Surgeons: A 2-year Prospective Study. *Radiology.* 2016:152004.
2. Boiselle PM, Biederer J, Gefter WB, Lee EY. Expert opinion: why is MRI still an under-utilized modality for evaluating thoracic disorders? *J Thorac Imaging.* 2013;28(3):137.
3. Ackman JB, Wu CC, Halpern EF, Abbott GF, Shepard JA. Nonvascular thoracic magnetic resonance Imaging: The current state of training, utilization, and perceived value: Survey of the Society of Thoracic Radiology membership. *J Thorac Imaging.* 2014;29(4):252-257.
4. Marks B, Mitchell DG, Simelaro JP. Breath-holding in healthy and pulmonary-compromised populations: effects of hyperventilation and oxygen inspiration. *J Magn Reson Imaging.* 1997;7(3):595-597.
5. Carter BW, Tomiyama N, Bhora FY, et al. A modern definition of mediastinal compartments. *J Thorac Oncol.* 2014;9(9):S97-101.
6. Ackman JB, Verzosa S, Kovach AE, et al. High rate of unnecessary thymectomy and its cause. Can computed tomography distinguish thymoma, lymphoma, thymic hyperplasia, and thymic cysts? *Eur J Radiol.* 2015;84(3):524-533.
7. Baron RL, Lee JK, Sagel SS, Peterson RR. Computed tomography of the normal thymus. *Radiology.* 1982;142(1):121-125.
8. Ackman JB, Kovacina B, Carter BW, et al. Sex difference in normal thymic appearance in adults 20-30 years of age. *Radiology.* 2013;268(1): 245-253.
9. Inaoka T, Takahashi K, Mineta M, et al. Thymic hyperplasia and thymus gland tumors: differentiation with chemical shift MR imaging. *Radiology.* 2007;243(3):869-876.
10. Priola AM, Priola SM, Ciccone G, et al. Differentiation of rebound and lymphoid thymic hyperplasia from anterior mediastinal tumors with dual-echo chemical-shift MR imaging in adulthood: reliability of the chemical-shift ratio and signal intensity index. *Radiology.* 2015;274(1):238-249.
11. Ackman JB, Mino-Kenudson M, Morse CR. Nonsuppressing normal thymus on chemical shift magnetic resonance imaging in a young woman. *J Thorac Imaging.* 2012;27(6):W196-198.
12. McInnis MC, Flores EJ, Shepard JA, Ackman JB. Pitfalls in the Imaging and Interpretation of Benign Thymic Lesions: How Thymic MRI Can Help. *AJR Am J Roentgenol.* 2016;206(1):W1-8.
13. Merine DS, Fishman EK, Zerhouni EA. Computed tomography and magnetic resonance imaging diagnosis of thymic cyst. *J Comput Tomogr.* 1988;12(3):220-222.
14. Takahashi K, Al-Janabi NJ. Computed tomography and magnetic resonance imaging of mediastinal tumors. *J Magn Reson Imaging.* 2010;32(6):1325-1339.
15. Molina PL, Siegel MJ, Glazer HS. Thymic masses on MR imaging. *AJR Am J Roentgenol.* 1990;155(3):495-500.
16. Tateishi U, Muller NL, Johkoh T, et al. Primary mediastinal lymphoma: characteristic features of the various histological subtypes on CT. *J Comput Assist Tomogr.* 2004;28(6):782-789.
17. Sakai S, Murayama S, Soeda H, Matsuo Y, Ono M, Masuda K. Differential diagnosis between thymoma and non-thymoma by dynamic MR imaging. *Acta Radiol.* 2002;43(3):262-268.
18. Sadohara J, Fujimoto K, Muller NL, et al. Thymic epithelial tumors: comparison of CT and MR imaging findings of low-risk thymomas, high-risk thymomas, and thymic carcinomas. *Eur J Radiol.* 2006;60(1):70-79.
19. Razek AA, Elmorsy A, Elshafey M, Elhadedy T, Hamza O. Assessment of mediastinal tumors with diffusion-weighted single-shot echo-planar MRI. *J Magn Reson Imaging.* 2009;30(3):535-540.
20. Rosado-de-Christenson ML, Templeton PA, Moran CA. From the archives of the AFIP. Mediastinal germ cell tumors: radiologic and pathologic correlation. *Radiographics.* 1992;12(5): 1013-1030.
21. Patel IJ, Hsiao E, Ahmad AH, Schroeder C, Gilkeson RC. AIRP best cases in radiologic-pathologic correlation: mediastinal mature cystic teratoma. *Radiographics.* 2013;33(3):797-801.
22. Rosado-de-Christenson ML, Pugatch RD, Moran CA, Galobardes J. Thymolipoma: analysis of 27 cases. *Radiology.* 1994;193(1):121-126.
23. Hahn HP, Fletcher CD. Primary mediastinal liposarcoma: clinicopathologic analysis of 24 cases. *Am J Surg Pathol.* 2007;31(12):1868-1874.
24. Munden RF, Nesbitt JC, Kemp BL, Chasen MH, Whitman GJ. Primary liposarcoma of the mediastinum. *AJR Am J Roentgenol.* 2000;175(5):1340.
25. Fitch SJ, Tonkin IL, Tonkin AK. Imaging of foregut duplication cysts. *Radiographics.* 1986;6(2):189-201.
26. Jeung MY, Gasser B, Gangi A, et al. Imaging of cystic masses of the mediastinum. *Radiographics.* 2002;22 Spec No:S79-93.
27. Takeda S, Miyoshi S, Minami M, Ohta M, Masaoka A, Matsuda H. Clinical spectrum of mediastinal cysts. *Chest.* 2003;124(1):125-132.
28. Cole TJ, Turner MA. Manifestations of gastrointestinal disease on chest radiographs. *Radiographics.* 1993;13(5):1013-1034.
29. Jang KM, Lee KS, Lee SJ, et al. The spectrum of benign esophageal lesions: imaging findings. *Korean journal of radiology : official journal of the Korean Radiological Society.* 2002;3(3):199-210.
30. Riddell AM, Hillier J, Brown G, et al. Potential of surface-coil MRI for staging of esophageal cancer. *AJR Am J Roentgenol.* 2006;187(5): 1280-1287.
31. Balcombe J, Torigian DA, Kim W, Miller WT, Jr. Cross-sectional imaging of paragangliomas of the aortic body and other thoracic branchiomeric paraganglia. *AJR Am J Roentgenol.* 2007;188(4):1054-1058.
32. Nakazono T, White CS, Yamasaki F, et al. MRI findings of mediastinal neurogenic tumors. *AJR Am J Roentgenol.* 2011;197(4):W643-652.
33. Olsen WL, Dillon WP, Kelly WM, Norman D, Brant-Zawadzki M, Newton TH. MR imaging of paragangliomas. *AJR Am J Roentgenol.* 1987;148(1):201-204.
34. Sherrick AD, Brown LR, Harms GF, Myers JL. The radiographic findings of fibrosing mediastinitis. *Chest.* 1994;106(2):484-489.
35. Brown LR, Reiman HM, Rosenow EC, 3rd, Gloviczki PM, Divertie MB. Intrathoracic lymphangioma. *Mayo Clin Proc.* 1986;61(11):882-892.
36. Semelka RC, Brown ED, Ascher SM, et al. Hepatic hemangiomas: a multi-institutional study of appearance on T2-weighted and serial gadolinium-enhanced gradient-echo MR images. *Radiology.* 1994;192(2):401-406.
37. Cheung YC, Ng SH, Wan YL, Tan CF, Wong HF, Ng KK. Dynamic CT features of mediastinal hemangioma: more information for evaluation. *Clin Imaging.* 2000;24(5):276-278.
38. Goshima S, Kanematsu M, Watanabe H, et al. Hepatic hemangioma and metastasis: differentiation with gadoxetate disodium-enhanced 3-T MRI. *AJR Am J Roentgenol.* 2010;195(4): 941-946.
39. McAdams HP, Rosado-de-Christenson ML, Moran CA. Mediastinal hemangioma: radiographic and CT features in 14 patients. *Radiology.* 1994;193(2):399-402.
40. Ackman JB. MR Imaging of Mediastinal Masses. *Magn Reson Imaging Clin N Am.* 2015;23(2):141-164.
41. Tanaka O, Kiryu T, Hirose Y, Iwata H, Hoshi H. Neurogenic tumors of the mediastinum and chest wall: MR imaging appearance. *J Thorac Imaging.* Vol 20. 2005/11/12 ed2005:316-320.